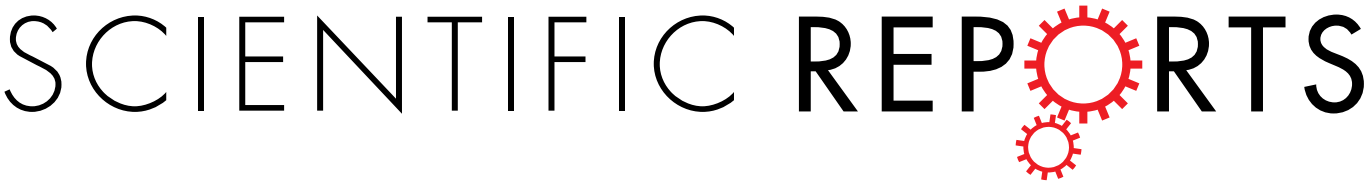

OPEN

Corrosion inhibition of mild steel in sulfuric acid solution by loquat (Eriobotrya japonica Lindl.) leaves extract

Received: 21 December 2016
Accepted: 24 May 2018
Published online: 14 June 2018

Xingwen Zheng[1,2], Min Gong[2], Qiang Li[1] & Lei Guo[3]

The inhibition performance and mechanism of loquat leaves extract (LLE) for the corrosion of mild steel in 0.5 M H_2SO_4 were investigated using weight loss method, electrochemical measurements and scanning electron microscope (SEM). The results revealed that LLE acted as a modest cathodic inhibitor, its inhibition efficiency increased with the concentration of LLE and reached a maximum value of 96% at the 100% V/V concentration, but decreased with incremental temperature. Besides, it was found that the adsorption of LLE on steel surface obeyed Langmuir adsorption isotherm, and then the thermodynamic and kinetic parameters were further determined accordingly. Furthermore, LLE was preliminarily separated by pH-gradient sedimentation and the synergistic inhibition between the isolates was investigated.

In recent years, plant extracts as corrosion inhibitors have attracted extensive attention due to their properties of environment-friendliness, low cost and renewability[1–3]. Notably, the first patented corrosion inhibitors applied for restraining iron corrosion in acid media are either natural products such as flour, yeast etc., or byproducts of food industries[4–7]. Recently, hundreds of plant extracts have been reported as inhibitors for steel in acid solutions[1–3,7–32]. For instance, Li *et al.*[1,8,9] studied the corrosion inhibition of steel by eco-friendly bamboo leaves extract in HCl, H_2SO_4, H_3PO_4, and citric acid solution. Lebrini *et al.*[17,26] noticed of steel corrosion inhibition in hydrochloric acid medium by alkaloids extracted from Oxandra asbeckii plant as well as Aniba rosaeodora plant. In addition, plant extracts have also been reportedly used as corrosion inhibitors for other metal and alloy, including Aloe vera[33] and Mansoa alliacea[34] for zinc, Mimosa[35] and Camellia sinensis[36] for brass, Morinda tinctoria[37] and Myrtus communis[38] for copper, and Spondias mombin L.,[39] Jasminum nudiflorum Lindl.,[40] Gossipium hirsutum L.[41] and Date palm[42] for aluminum. However, compared with the huge number of plant resources and the potential demand for efficient green corrosion inhibitors, more research is still needed. And, the phytochemical investigations to the effective inhibitive composition of plant extract are still scarce, which has important significance for understanding the inhibition mechanism of plant extract and the development of new inhibitors.

Eriobotrya japonica Lindl. (loquat) is a flowering plant belonging to the Rosaceae family and widely distributed in East Asia including China, Korea, Japan and many other countries[43–45]. This paper reports the effect of acid extract of loquat leaves as an environmentally friendly corrosion inhibitor for mild steel in 0.5 M H_2SO_4 using gravimetric technique, potentiodynamic polarization, electrochemical impedance spectroscopy (EIS) and microscopic examination. Moreover, LLE was preliminarily separated by pH-gradient sedimentation, thus the isolates were characterized through high performance liquid chromatograph (HPLC), mass spectrometry (MS), amino acid analyzer and Fourier transform infrared spectroscopy (FTIR), and the synergistic inhibition between the isolates was investigated.

Results and Discussion

The curves of open circuit potential (OCP) versus time are depicted in Figure 1, it could be seen that the OCP of steel electrode in the studied solutions nearly reached a steady level after immersion for 30 minutes, and the

[1]School of Chemical and Environmental Engineering, Sichuan University of Science & Engineering, Zigong, 643000, China. [2]Key Laboratory of Material Corrosion and Protection of Sichuan Province, Zigong, 643000, China. [3]School of Materials and Chemical Engineering, Tongren University, Tongren, 554300, China. Correspondence and requests for materials should be addressed to X.Z. (email: zxwasd@126.com)

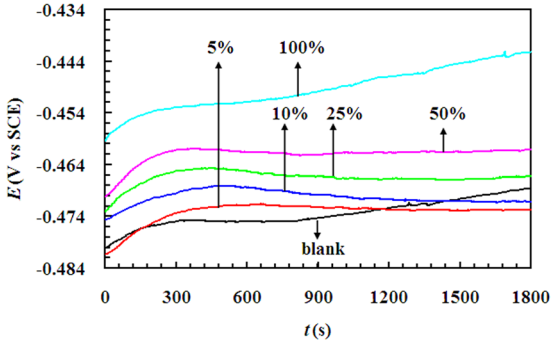

Figure 1. The OCP-time curves for mild steel in 0.5 M H_2SO_4 solution containing different different V/V concentrations of LLE at 298 K.

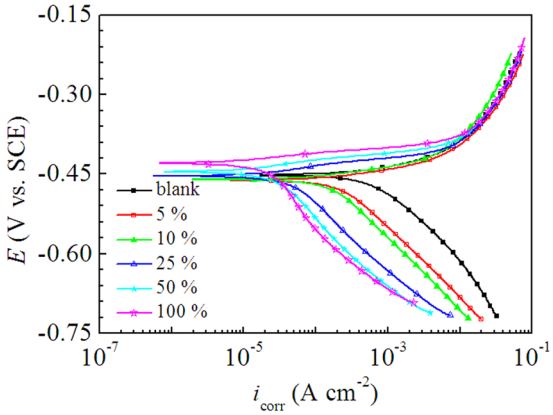

Figure 2. Potentiodynamic polarization curves of mild steel in 0.5 M H_2SO_4 solutions without and with different V/V concentrations of LLE at 298 K.

c(% V/V)	E_{corr} (V vs. SCE)	I_{corr}(mA cm^{-2})	$-\beta_c$(mV dec^{-1})	η(%)
blank	−0.452	0.578	123.1	\
5	−0.462	0.202	126.6	65.0
10	−0.460	0.145	130.7	74.9
25	−0.453	0.043	138.6	92.5
50	−0.446	0.028	157.1	95.2
100	−0.429	0.021	192.7	96.3

Table 1. The electrochemical parameters for mild steel in 0.5 mol/L H_2SO_4 solution without and with different V/V concentrations of LLE at 298 K.

values of OCP, taking the average of the last 600 seconds, were −0.4706, −0.4728, −0.4711, −0.4667, −0.4615 and −0.4446 V vs. SCE for LLE V/V concentrations of 0, 5, 10, 25, 50 and 100%, respectively.

Figure 2 illustrates the potentiodynamic polarization curves of mild steel in 0.5 M H_2SO_4 solutions containing different concentrations of LLE at 298 K. As shown in Figure 2, since there was no linear Tafel region on anodic polarization curve, thus the electrochemical parameters, including corrosion potential (E_{corr}), corrosion current density (I_{corr}), cathodic Tafel slope (β_c) and inhibition efficiency (η), were determined by extrapolation of the cathodic part of the polarization curve to E_{corr}, and listed in Table 1. Figure 2 and Table 1 show that the presence of LLE caused a remarkable decrease of I_{corr} value, and a higher concentration of LLE resulted in an even lower I_{corr} value. Accordingly, the inhibition efficiency increased along with the increase of LLE concentration, and the maximum inhibition efficiency reached 96% at the 100% V/V concentration. Moreover, Figure 2 also indicates that the addition of LLE prominently shifted the cathodic branch of polarization curves to lower values of current densities, suggesting strong inhibitive effect of LLE on the cathodic reduction of hydrogen ions. Besides, it can be observed from in Figure 2 that the cathodic polarization curves were almost parallel to each other, the values of β_c in Table 1 exhibited small fluctuations accordingly, which indicate that LLE dose not impact the mechanism of hydrogen reduction and the hydrogen evolution is activation-controlled[46]. However, the anodic polarization curve with inhibitor almost overlapped with that in the blank solution in the strong polarization region, despite

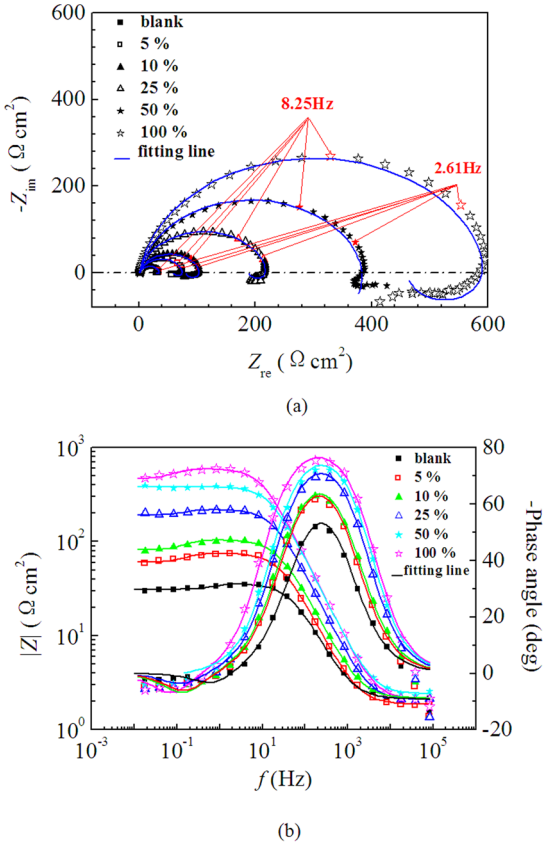

Figure 3. Nyquist plots (**a**) and Bode plots (**b**) for mild steel in 0.5 M H_2SO_4 solution without and with different V/V concentrations of LLE at 298 K.

small decrease of anodic current density at low polarization potential, which is attributed to the desorption of inhibitors. Besides, the values of E_{corr} did not vary significantly with a displacement less than 30 mV (as seen in Table 1). Overall, LLE can be seen as a modest cathodic inhibitor[47,48].

Figure 3 shows the Nyquist plots and Bode plots for mild steel in 0.5 M H_2SO_4 solution without and with different concentrations of LLE at 298 K. It can be seen that the addition of LLE did not change the profile of Nyquist plots, which consist of a capacitive loop at high frequencies (HF) and an inductive loop at low frequencies (LF), suggesting that the presence of the LLE has little influence on the corrosion mechanism[1,11]. The HF capacitive loop is usually related to the charge transfer of the corrosion process and the resultant double layer behavior[49–51]. However, due to the frequency dispersion as a result of the roughness and non-homogeneity of electrode surface[52], the capacitive loop exhibits a depressed semicircle. Meanwhile, the LF inductive loop is attributed to the relaxation process caused by adsorption of species such as $(SO_4^{2-})_{ads}$ and $(H^+)_{ads}$[48,51]. Figure 3b shows the impedance data in the Bode plots of impedance magnitude (|Z|) and phase angle over the whole frequency range obtained for the mild steel electrode with LLE V/V concentrations between 0 and 100%. The phase angles of the uninhibited and inhibited solutions are 52.3°, 61.6°, 62.8°, 69.9°, 72.9° and 75.7°, respectively, the values of phase angle and impedance magnitude at LF increase with the increase of LLE concentration, which indicates better protection behavior of LLE with higher concentrations.

The EIS data are simulated with the equivalent circuits as shown in Figure 4 using the ZSimpWin software and the impedance parameters are given in Table 2. In the circuits, R_s, R_{ct} and R_L represent the solution resistance, charge transfer resistance and inductive resistance, respectively, L is the inductive elements, and constant phase element (CPE) is used to replace a double layer capacitance in order to obtain a better fitting. The impedance of CPE can be described as follows[52,53]:

$$Z_{CPE} = \frac{1}{Y_0(j\omega)^n} \tag{1}$$

where Y_0 is the CPE constant, j is the imaginary unit, ω is the angular frequency, and n is the deviation parameter, has the meaning of the phase shift. In addition, the double layer capacitance (C_{dl}) and inhibition efficiency (η) are calculated according to the following equations[52,53]:

$$C_{dl} = Y_0(\omega)^{n-1} = Y_0(2\pi f_{z_{im}-Max})^{n-1} \tag{2}$$

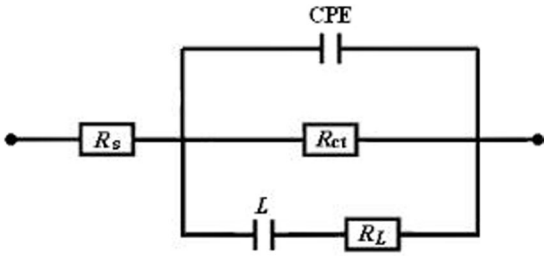

Figure 4. Equivalent circuits used to fit the EIS.

C (% V/V)	R_s (Ω cm²)	$Y_0 \times 10^{-6}$ (S s^n cm^{-2})	n	R_{ct} (Ω cm²)	C_{dl} (μF cm^{-2})	L (Ω cm²)	R_L (Ω cm²)	η (%)
blank	2.1	202.0	0.87	34	96.6	46	193	\
5	1.9	143.1	0.89	74	81.7	323	276	54.1
10	2.2	117.4	0.88	103	65.1	429	343	67.0
25	2.1	62.7	0.91	219	41.0	1741	1359	84.5
50	2.4	40.5	0.92	384	28.2	3124	2624	91.1
100	2.1	37.9	0.92	596	27.6	4850	2023	94.3

Table 2. The EIS parameters for mild steel in 0.5 mol/L H_2SO_4 solution without and with different V/V concentrations of LLE at 298 K.

$$\eta = \frac{R_{ct} - R_{ct,0}}{R_{ct}} \times 100 \quad (3)$$

where ω is the angular frequency at the maximum value of the imaginary part ($Z_{im\text{-}Max}$) of the impedance spectrum[52], $R_{ct,0}$ and R_{ct} are the charge transfer resistances without and with inhibitor, respectively.

As shown in Table 2, the R_{ct} values increased while the values of C_{dl} declined when increasing LLE concentration, correspondingly, the inhibition efficiency increased with the increase of the concentration of LLE, which indicate that the inhibitor molecules adsorbed at the metal/solution interface as a barrier layer, effectively protecting the mild steel from aggressive attack by the acid solution. The values of *n* became closer to one as the increase of LLE concentration, indicating the metal surface become more homogeneous due to the adsorption of inhibitor molecules[1].

The results of weight loss measurements for the corrosion of mild steel in 0.5 M H_2SO_4 solution without and with different concentrations of LLE for 4 h at different temperatures are given in Table 3. It is clear that the corrosion rate decreases under the same temperature when increasing inhibitors concentration, while it increases with rising of temperature, additionally, the inhibition efficiency at same concentration of inhibitor also decreased at higher temperature. At the 100% V/V concentration, the inhibition efficiency of LLE reached maximum value of 96.2, 95.0, 89.5 and 89.2% for 298, 308, 318 and 328 K, respectively, which mean LLE is an effective inhibitor for the corrosion of mild steel in 0.5 M H_2SO_4 solution. In addition, the inhibition efficiencies obtained from weight loss measurements are in good agreement with those obtained by electrochemical measurements.

Moreover, the inhibition efficiency of LLE is compared with that of other plant extract reported in literature[2,28,54–60], the related data are listed in Table 4. It can be seen that the inhibition efficiency of LLE is slightly less than that of Radish seed extract at the V/V concentration of 10%, and compared with the maximum corrosion inhibition efficiency reported in the literature, the inhibition efficiency of LLE is close to that of Houttuynia cordata stem extract and Barley extract, slightly lower than that of Agetes erecta extract and Litchi peel extract, but higher than that of the extract of Medicago sativa, Anacyclus pyrethrum extract, Salvia aucheri mesatlantica, and so on, which suggest that LLE is an effective inhibitor.

It is well known that the inhibition effect of organic inhibitor is based on their adsorption at the metal/solution interfaces, therefore, it is important to understand the adsorption behavior of inhibitor for revealing its inhibition mechanism. The adsorption isotherm can provide vital information regarding the interaction between the inhibitor and the metal surface. Thus, several adsorption isotherms are employed to fit the surface coverage (θ) obtained from weight loss measurements. Langmuir isotherm is found to provide the optimal description of the adsorption behavior of LLE on the mild steel surface, which can be expressed by the following equation[61,62]:

$$\frac{c}{\theta} = \frac{1}{K_{ads}} + c \quad (4)$$

where *c* is the inhibitor concentration, θ is the surface coverage and K_{ads} is the adsorptive equilibrium constant, respectively.

T(K)	c(% V/V)	v(g m^{-2} h^{-1})	η(%)	θ
298	blank	13.54	/	/
	5	3.86	71.5	0.715
	10	2.57	81.1	0.811
	25	1.98	85.4	0.854
	50	1.22	91.0	0.910
	100	0.52	96.2	0.962
308	blank	25.42	/	/
	5	7.72	69.6	0.696
	10	5.48	78.4	0.784
	25	3.93	84.6	0.845
	50	2.91	88.5	0.885
	100	1.28	95.0	0.950
318	blank	37.92	/	/
	5	16.05	57.7	0.577
	10	11.27	70.3	0.703
	25	9.10	76.0	0.760
	50	6.23	83.6	0.836
	100	3.98	89.5	0.895
328	blank	60.89	/	/
	5	40.65	33.2	0.332
	10	23.23	61.9	0.619
	25	16.20	73.4	0.734
	50	10.05	83.5	0.835
	100	6.57	89.2	0.892

Table 3. Corrosion parameters obtained from weight loss measurements for mild steel in 0.5 M H_2SO_4 solution without and with different V/V concentrations of LLE for 4 h at different temperatures.

Plant extract	C^1	η(%)^2	T(K)	Reference
LLE	10% V/V	81.1/67.0/74.9	298	this work
Radish seed extract [3]	10% V/V	−/80.2/79.3	303	[28]
LLE	100% V/V	96.2/94.3/96.3	298	this work
Medicago sativa leaf	500 ppm	50.0/ – /92.0	298	[54]
Houttuynia cordata stem	3.0 g/L	98.3/94.8/94.4	298	[55]
Anacyclus pyrethrum leaf and stem	350 mg/L	−/87.0/82.0	303	[56]
Anacyclus pyrethrum flower	350 mg/L	−/88.9/84.3	303	[56]
Anacyclus pyrethrum root	350 mg/L	−/79.3/79.9	303	[56]
Barley	0.84 g/L	−/94.2/94.6	303	[57]
Agetes erecta (Marigold flower)	1.0 g/L	96.3/98.1/98.2	303	[2]
Litchi (Litchi Chinensis) peels	3.0 g/L	−/97.8/95.7	298	[58]
Aerial part of Salvia aucheri mesatlantica	2.0 g/L	70.1/84.2/85.5	298 [4]	[59]
Coconut coir dust	0.5 g/L	87.0/94.3/66.5	303	[60]

Table 4. The inhibition efficiency of LLE on the corrosion of steel in 0.5 M H_2SO_4 solution compared with that of other extract described in literature. NOTE: [1]Concentration corresponding to the maximum corrosion inhibition efficiency. [2]The inhibition efficiency was listed in the order as follows: weight loss, electrochemical impedance spectroscopy and potentiodynamic polarization. [1]The inhibition efficiency was tested in 1 M H_2SO_4 solution. [4]The temperature of weight loss method is 303 K.

The plots of c/θ versus c yield a straight line at different temperature as shown in Figure 5, confirming that the adsorption of LLE on the mild steel in 0.5 M H_2SO_4 solution obeys Langmuir isotherm. From the intercepts of the straight lines in Figure 5, the values of K_{ads} at different temperatures were calculated and listed in Table 5. The K_{ads} values decreased with the increase of temperature, which corresponded to the reduction of inhibition efficiency with rising temperature. Moreover, the adsorption enthalpy (ΔH^0_{ads}) can be calculated using Van't Hoff equation[62]:

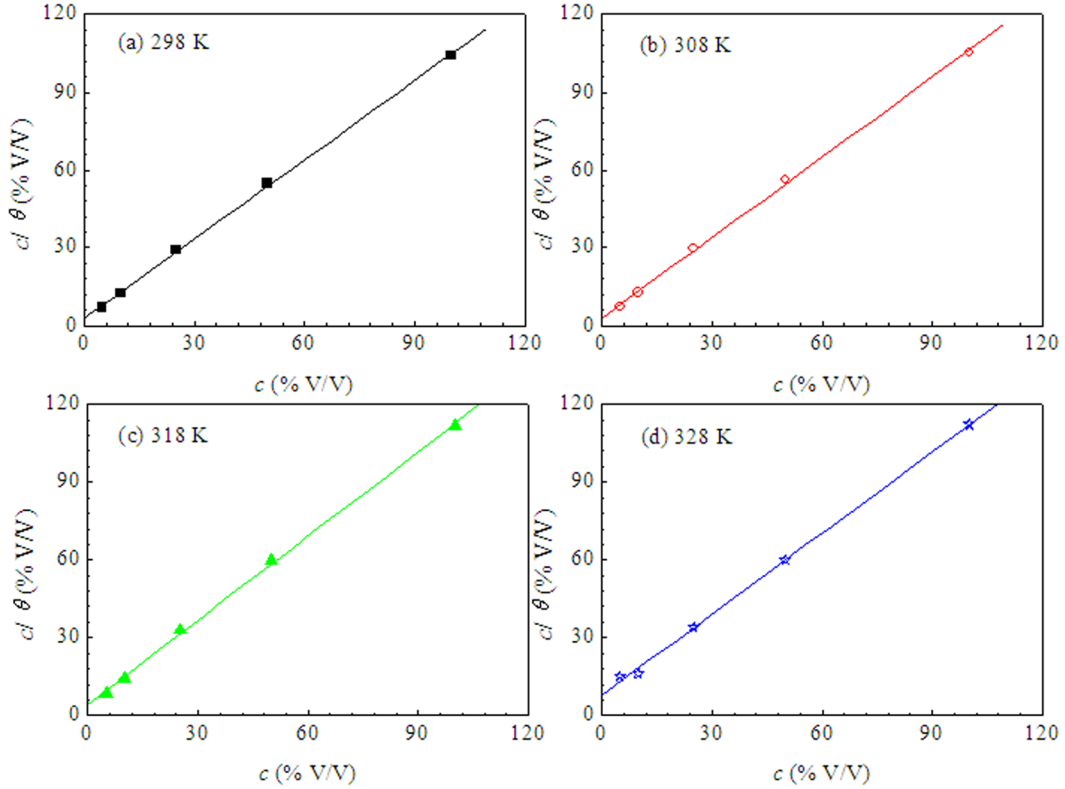

Figure 5. Langmuir isotherm plots for mild steel in 0.5 M H_2SO_4 solution containing different V/V concentrations of LLE at different temperature.

T(K)	K_{ads}(1/%)	ΔH^0_{ads} (kJ/mol)
298	0.363	−31.34
308	0.333	
318	0.232	
328	0.127	

Table 5. The thermodynamic parameters for mild steel in 0.5 M H_2SO_4 solution containing different V/V concentrations of LLE at different temperature.

$$\ln K_{ads} = -\frac{\Delta H^0_{ads}}{RT} + \text{constant} \tag{5}$$

where R is the universal gas constant, T is the thermodynamic temperature. Figure 6 shows that there is a linear relationship between $\ln K_{ads}$ and $1000/T$, thus the value of ΔH^0_{ads} is calculated according to the Equation (5) and listed in Table 5, the negative value of ΔH^0_{ads} suggests the adsorption of the effective inhibitor component in LLE onto the mild steel surface is an exothermic process[62,63].

Temperature is an important factor affecting the performance of inhibitor, and Table 3 indicates that the inhibition efficiency of LLE decreased with rising of temperature. To further understand the inhibitive mechanism of LLE, Arrhenius equation and transition state equation were employed to fit the corrosion rates at different temperatures. The two equations can be expressed respectively as follows[61,62]:

$$\ln \nu = -\frac{E_a}{RT} + \ln A \tag{6}$$

$$\ln \frac{\nu}{T} = \ln \frac{R}{Nh} + \frac{\Delta S_a}{R} - \frac{\Delta H_a}{RT} \tag{7}$$

where ν is the corrosion rate obtained from weight loss measurements, A is the pre-exponential factor, h is the Plank's constant, N is the Avogadro's number, E_a is the apparent activation energy, ΔS_a is the apparent entropy of activation, ΔH_a is the apparent enthalpy of activation. Correspondingly, the fitting results are shown in Figure 7, the

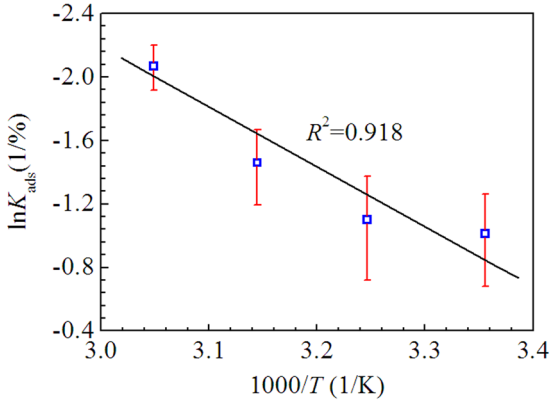

Figure 6. The relationship between $\ln K_{ads}$ and (1000/T) for mild steel in 0.5 M H_2SO_4 solution containing LLE.

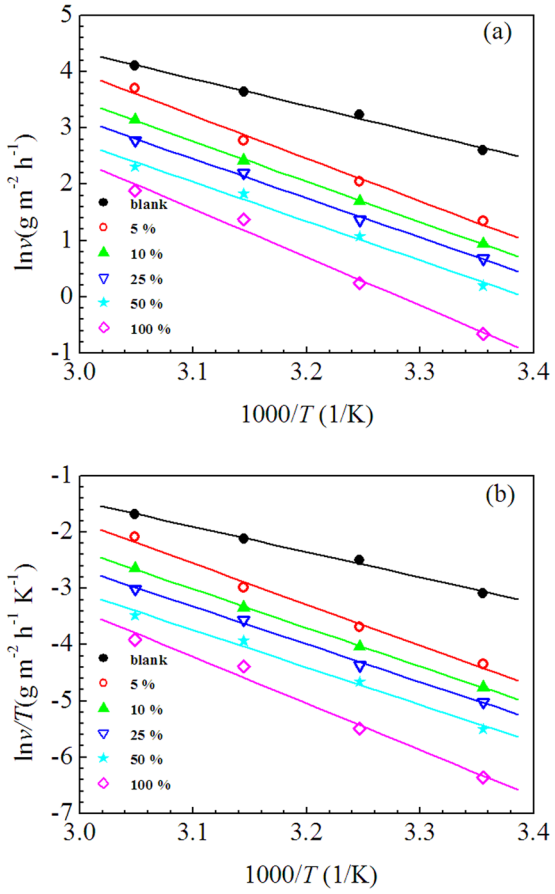

Figure 7. Arrhenius plots (**a**) and Transition state plots (**b**) for mild steel in 0.5 M H_2SO_4 solution in the absence and presence of various V/V concentrations of LLE.

plots in Figure 7 present straight lines, thus according to the slopes and intercepts of these straight lines, the kinetic parameters including E_a, ΔH_a and ΔS_a, are calculated and listed in Table 6. The value of E_a is greater in 0.5 M H_2SO_4 solution containing LLE than that in blank solution, which indicate that the adsorption of LLE on the mild steel surface leads to the dissolution of steel become difficult. And just as expected, the values of E_a and ΔH_a follow the same trend of variation with the concentration of LLE, according to the transition state theory, $\Delta H_a = E_a - RT$[64]. Additionally, Table 6 shows that the values of ΔS_a is more positive in inhibited solution compared to that in blank solution, which indicate the system disorder increased from reactant to activated complex during the corrosion process[48,65].

The SEM micrographs of mild steel samples after immersed in blank solution and in inhibited solutions for 4 h at 298 K are shown in Figure 8. As shown in Figure 8a, in the absence of LLE, the mild steel surface is fairly

c(% V/V)	E_a(kJ/mol)	ΔH_a(kJ/mol)	ΔS_a(J K^{-1} mol^{-1})
blank	39.96	37.36	−97.55
5	63.21	60.62	−30.87
10	59.55	56.96	−46.04
25	58.08	55.48	−53.19
50	57.85	55.25	−57.33
100	71.25	68.65	−19.76

Table 6. Activation p.arameters for mild steel in 0.5 M H_2SO_4 solution in the absence and presence of various V/V concentrations of LLE.

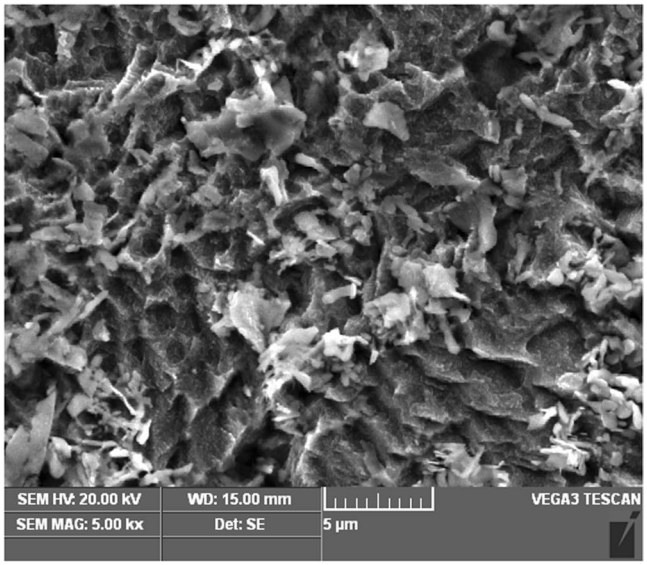

(a)

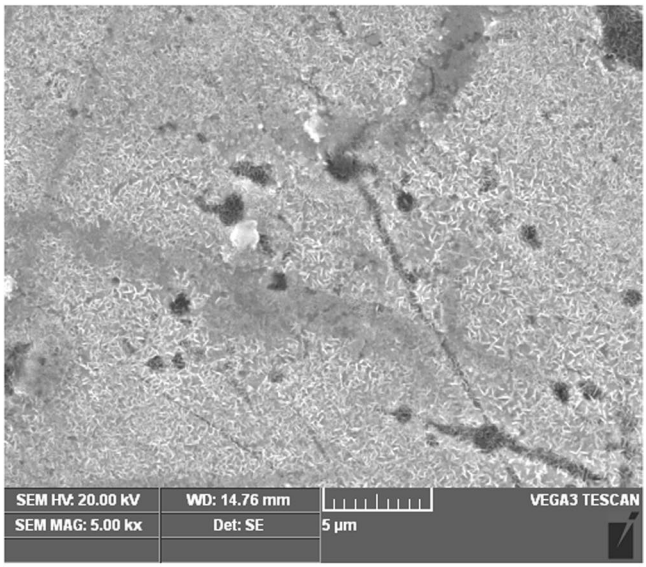

(b)

Figure 8. SEM micrographs of mild steel surface after immersed in 0.5 M H_2SO_4 solution in the absence of LLE (**a**) and in presence of 100% V/V LLE (**b**) for 4 h at 298 K.

rough and seriously damaged by the aggressive solution. In comparison, in presence of 100% V/V LLE, the steel surface is lightly damaged, which indicate the addition of LLE can effectively inhibit the corrosion of mild steel in the aggressive H_2SO_4 solution.

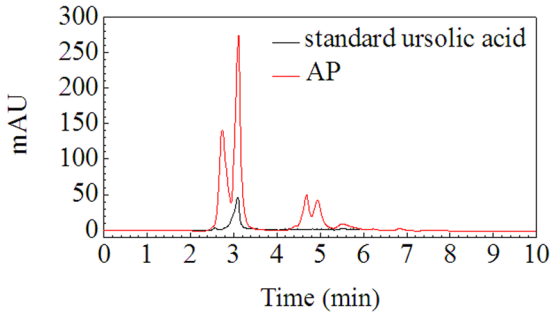

Figure 9. HPLC chromatograms of standard ursolic acid and AP.

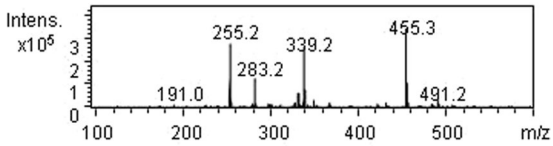

Figure 10. MS of AP.

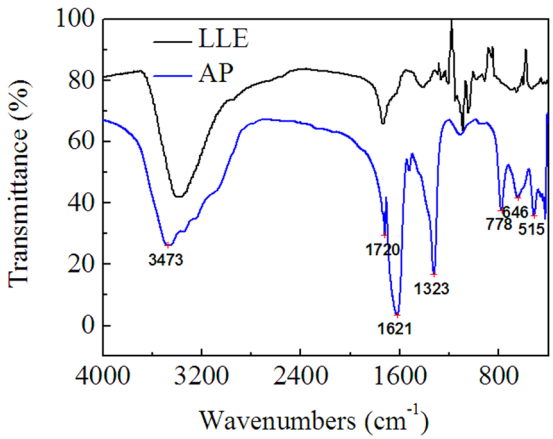

Figure 11. FTIR spectra of AP and the differential infrared spectroscopy of LLE.

By pH-gradient sedimentation, LLE was preliminarily separated into acidic precipitate (AP), alkali precipitate (BP) and remaining solution (RS). HPLC chromatograms of standard ursolic acid and AP are shown in Figure 9, which indicate that ursolic acid is present in AP, but AP is not pure substance. This result is further confirmed by the MS of AP shown in Figure 10, in which, the quasimolecular ions $[M-H]^-$ at *m/z* 191.0, 255.2 and 455.3 are in agreement with citric acid[66], palmitic acid[67] and ursolic acid[67,68]. Figure 11 shows the FTIR spectra of AP and the differential infrared spectra of LLE. The differential spectroscopy was obtained through the FTIR spectra of stock solution of LLE and the sulfuric acid solution using software OMNIC 7.0 by differential spectroscopic analysis. It is clearly seen that the infrared absorption peaks of AP are basically in accordance with those of LLE, indicating that AP is the main component of the LLE. Combined with the results of MS, the strong and broad peak at 3473 cm^{-1} can be attributed to the stretching vibrations of hydroxyl (OH) or carboxyl (COOH) groups, the peaks at 1720 cm^{-1} and 1621 cm^{-1} are the characteristic peaks of O = C and C = C, respectively[69,70]. Absorption peak at 1323 cm^{-1} may be indicate C-H bending vibration[69], and the peaks at 778, 646, 515 cm^{-1} could be assigned to C-H of aliphatic and aromatic carbon. Figure 12 shows the HPLC chromatogram and MS of BP, then comparing mass spectrometric data with literatures, the peak at *m/z* 477.4 was consistent with the presence of isorhamnetin 3-O-galactoside or isorhamnetin-3-O-glucoside[43], while the molecular ion at *m/z* 451.3 was identified as cinchonain Ia[69] or cinchonain Ib[71,72]. The peak with $[M-H]^-$ at *m/z* 519.4 probably produced by lignan of (+)-Pinoresinol-O-β-D-glucopyranoside[73] or dehydrodiconiferylalcohol-9′-O-β-D-glucopyranoside[74]. The FTIR of BP is shown in Figure 13, the absorption peaks of 3434 and 1626 cm^{-1} are attributed to the stretching vibrations of hydroxyl and C = C, respectively[69,70], the peak at 1417 cm^{-1} can be assigned to the bending vibrations of C-H or O-H[31], the adsorption band 1473 cm^{-1} corresponds to the stretching vibration of C-O[69], and the peak 569 cm^{-1} may be assigned to C-H of aliphatic and aromatic carbon. Consequently, the infrared absorption of

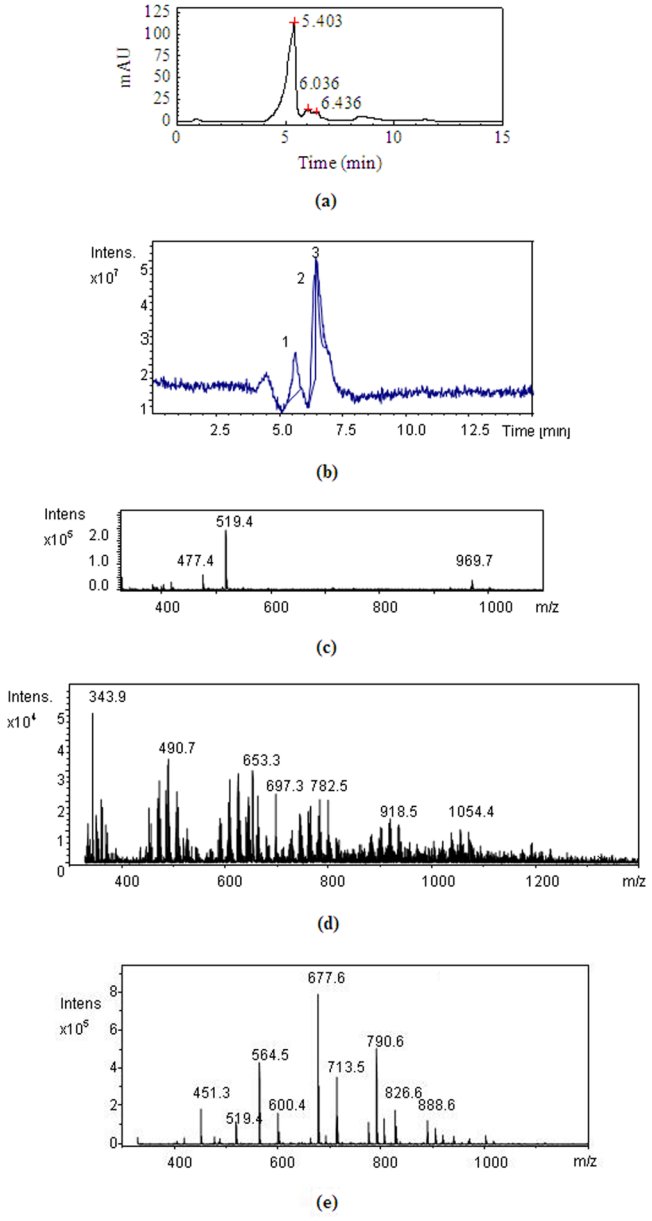

Figure 12. HPLC chromatograms of BP (**a**), total MS of BP (**b**), MS of BP at 4.3–4.7 min (**c**), MS of BP at 5.3–5.9 min (**d**) and MS of BP at 6.1–6.4 min (**e**).

BP is corresponding to the analysis of MS. Seven acids, including valine, tyrosine, phenylalanine, lysine, histidine and arginine were detected in RS, similar results were also reported by Yokota *et al.*[75]. Moreover, the color of RS changed with the pH value of the solution, which implies that RS contained anthraquinones.

Furthermore, the inhibition performance of the isolates and their mixtures was evaluated with the V/V concentration of 50% as a reference, the corresponding polarization curves and electrochemical parameters are shown in Figure 14 and Table 7, respectively. The results showed that AP can not inhibit the corrosion of mild steel in H_2SO_4 solution, and the inhibitory effect of BP was very weak, however, RS exhibited obvious corrosion inhibition. It is particularly important to note that the inhibition efficiency increased significantly when the isolate was mixed, and the inhibition efficiency of the mixture of three isolates is as high as 91%, which indicate that there is a strong synergistic effect between the chemical components of LLE.

From the foregoing, the inhibition mechanism of LLE can be described as follows:

When the loquat leaves were immersed in H_2SO_4 solution, the organic compounds in the leaves, such as amino acids, organic acids, glycosides, and so on, were dissolved into the solution and were further protonated in strongly acidic solution. It is usually considered that the steel surface charges positive charge in acid solution[76,77], which means that the protonated substances are difficult to adsorb on the steel surface due to the electrostatic repulsion, but Solmaz's study found that the steel surface carries negative charge in HCl solution in the presence of inhibitors[78,79], which allows the positively charged inhibitor molecules directly adsorb on the steel surface

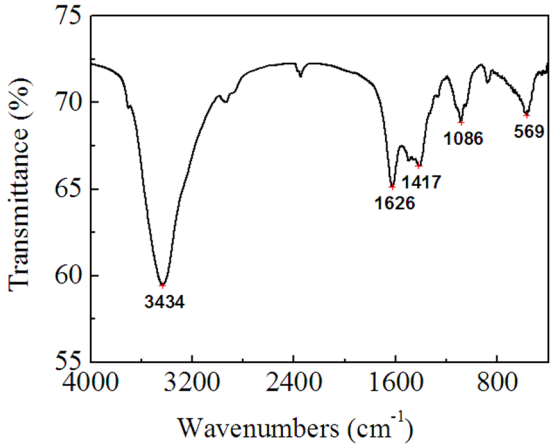

Figure 13. FTIR spectra of BP.

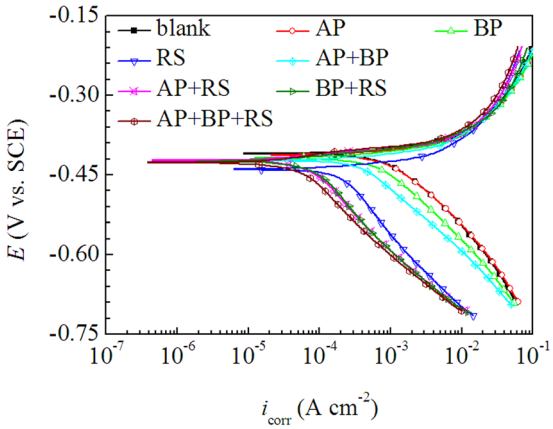

Figure 14. Potentiodynamic polarization curves for mild steel in 0.5 M H_2SO_4 solution without and with different isolates of LLE at 298 K.

c(% V/V)	E_{corr} (V vs. SCE)	I_{corr}(mA cm^{-2})	η(%)
blank	−0.409	0.611	\
AP	−0.412	0.676	\
BP	−0.417	0.589	3.7
RS	−0.432	0.204	66.7
AP + BP	−0.422	0.391	36.1
AP + RS	−0.422	0.070	88.6
BP + RS	−0.424	0.073	88.0
AP + BP + RS	−0.427	0.050	91.8

Table 7. The electrochemical parameters for mild steel in 0.5 mol/L H_2SO_4 solution without and with different isolates of LLE at 298 K.

through electrostatic interaction, and then reduce the steel dissolution. However, Figure 2 showed a weak inhibitory effect of LLE on the anodic dissolution of iron, which implies that the steel surface in the investigated solutions is positively charged or has very little negative charge. These protonated substances also can adsorb on cathodic sites of the steel in competition with hydrogen ions, maybe due to the higher adsorption rate of the positively charged inhibitor molecules than that of hydrogen ions, thus the cathodic reaction of hydrogen ions reduction can be inhibited[78,79], and the inhibitive effect of LLE on the cathodic reaction was clearly shown by polarization curves in Figure 2. As a result, LLE act as a modest cathodic inhibitor.

Methods

Electrolyte and Material. The corrosive solution 0.5 M H_2SO_4 was prepared using analytical grade sulphuric acid and distilled water. The chemical composition (in wt%) of mild steel as follows: C (0.16%), Si (0.18%), Mn (0.29%), P (0.014%), S (0.013%) and Fe for balance, and the preparation of specimens used in the experiments were the same as reported earlier[48–50]. Before conducting the test, the samples were mechanically abraded with emery paper up to 800 grit. During the experiment, the test solution was open to the air and under a static condition, meanwhile, temperature was controlled by a water thermostat with an accuracy of 1 K.

Preparation of Loquat Leaves Extract. Loquat leaves were picked up at the campus of Sichuan University of Science & Engineering in December 2014, and then rinsed well under running water before drying. The leaves were then kept in an oven at 50 °C for 72 h and ground to powder. And the powder was stored in a sealed container. Afterwards, the stock solution of loquat leaves extract (LLE) was prepared as follows: 100 g of powdered leaves were soaked in 1 L 0.5 M H_2SO_4 solutions for 12 h before the extract solution was filtered and stored. After that, the test solution with inhibitor, i.e. 5, 10, 25, 50 and 100% (V/V), were prepared through diluting the stock solution with corresponding amount of 0.5 M H_2SO_4 solution.

Isolation and characterization of LLE. LLE was first neutralized with sodium hydroxide, when the pH value of LLE increased to 1, white substance started to precipitate out, continuously adding alkali solution until before the color of LLE changes dramatically, at this point, the pH value of solution is about 5, after standing for 24 hours, the acidic precipitate of LLE (AP) was separated by centrifugation, then AP was washed three times with distilled water and dried in vacuum. While the remaining solution was continued alkalization, at pH 12, brown precipitate was found. The pH value of solution was adjusted to close to 14 in order to make precipitation more complete. Then alkali precipitation (BP) was obtained by centrifugation after the solution was stood for 24 h, and the remaining solution (RS) was neutralized with sulfuric acid and was not further isolated.

The methanol solution of AP was analyzed by Agilent 1100 high performance liquid chromatograph (HPLC) used ursolic acid as the reference substance, in which, the analytical column used was phenomenex C18, the mobile phase was methanol aqueous solution (90: 10, V/V) with a flow rate of 0.5 mL/min at 30 °C, and eluent was detected at 215 nm. Moreover, the composition of AP was further confirmed by mass spectrometry (MS). The composition of BP was detected by liquid chromatography-mass spectrometry (LC-MS) using Agilent LC1100/MSD-VL, and the chromatographic conditions were consistent with the foregoing. Furthermore, Hitachi L-8900 amino acid analyzer was employed to determine amino acids in RS, and FTIR spectra (KBr) was measured by Nicolet-6700 spectrophotometer.

Measurement Method. Electrochemical measurements were conducted in a three-electrode cell assembly with mild steel working electrode, saturated calomel electrode (SCE) and platinum electrode using CHI660E electrochemical work station (Shanghai Chenhua Instruments Co. Ltd., China). All potential data reported were referred to SCE reference electrode. The working electrode was initially immersed into test solution at OCP until it reached steady state. Then, EIS was measured at OCP. Ultimately, the polarization curve was obtained by potentiodynamic scanning method. The procedure for electrochemical measurements had been previously described in detail[48–50].

Weight loss measurements were performed in a wild-mouth glass bottle containing 500 mL of test solution for 4 h at different temperatures (298, 308, 318 and 328 K). After that, the microscopic examination of the specimen surface was performed using a Tescan Vega3 scanning electron microscopy at high vacuum. The experimental procedures and data processing were similar to previously reported researches[48–50].

Conclusions

(1) LLE can be considered as a modest cathodic inhibitor which mainly inhibits the cathodic process on the corrosion of mild steel in 0.5 M H_2SO_4 solution, and its inhibitive efficiency increases with the increment of LLE concentration, but decreases when rising temperature.
(2) In the presence of LLE, the charge transfer resistance increases while double layer capacitance declines, confirming the adsorption of inhibitor molecules on the mild steel surface. The adsorption of LLE on steel surface is an exothermic process and obeys Langmuir adsorption isotherm.
(3) The corrosion inhibition of LLE is caused by the combination of various components in the extract, and there is a synergistic effect between the components.

Data Availability. Te datasets generated during and/or analyzed during the current study are available from the corresponding author upon reasonable request.

References

1. Li, X., Deng, S., Xie, X. & Fu, H. Inhibition effect of bamboo leaves' extract on steel and zinc in citric acid solution. *Corros. Sci.* **87**, 15–26 (2014).
2. Mourya, P., Banerjee, S. & Singh, M. M. Corrosion inhibition of mild steel in acidic solution by Tagetes erecta (Marigold flower) extract as a green inhibitor. *Corros. Sci.* **85**, 352–363 (2014).
3. Li, L. *et al*. Adsorption and corrosion inhibition of Osmanthus fragran leaves extract on carbon steel. *Corros. Sci.* **63**, 82–90 (2012).
4. J. Baldwin, British Patent, 2327 (1895).
5. Putilova, N., Balezin, S. A. & Barannik, V. P. *Metallic Corrosion Inhibitors*. (Pergamon Press, Oxford, 1960).

6. Raja, P. B. & Sethuraman, M. G. Natural products as corrosion inhibitor for metals in corrosive media - A review. *Mater. Lett.* **62**, 113–116 (2008).
7. Okafor, P. C. *et al*. Inhibitory action of Phyllanthus amarus extracts on the corrosion of mild steel in acidic media. *Corros. Sci.* **50**, 2310–2317 (2008).
8. Li, X., Deng, S., Fu, H. & Xie, X. Synergistic inhibition effects of bamboo leaf extract/major components and iodide ion on the corrosion of steel in H_3PO_4 solution. *Corros. Sci.* **78**, 29–42 (2014).
9. Li, X., Deng, S. & Fu, H. Inhibition of the corrosion of steel in HCl, H_2SO_4 solutions by bamboo leaf extract. *Corros. Sci.* **62**, 163–175 (2012).
10. Ibrahim, T., Alayan, H. & Mowaqet, Y. A. The effect of Thyme leaves extract on corrosion of mild steel in HCl. *Prog. Org. Coat.* **75**, 456–462 (2012).
11. Gerengi, H. & Sahin, H. I. Schinopsis iorentzii extract as a green corrosion inhibitor for low carbon steel in 1 M HCl solution. *Ind. Eng. Chem. Res.* **51**, 780–787 (2012).
12. Deng, S. & Li, X. Inhibition by Ginkgo leaves extract of the corrosion of steel in HCl and H_2SO_4 solutions. *Corros. Sci.* **55**, 407–415 (2012).
13. Al-Otaibi, M. S. *et al*. Corrosion inhibitory action of some plant extracts on the corrosion of mild steel in acidic media. *Arab. J. Chem.* **7**, 340–346 (2014).
14. Eduok, U. M., Umoren, S. A. & Udoh, A. P. Synergistic inhibition effects between leaves and stem extracts of Sida acuta and iodide ion for mild steel corrosion in 1 M H_2SO_4 solutions. *Arab. J. Chem.* **5**, 325–337 (2012).
15. Ji, G., Shukla, S. K., Dwivedi, P., Sundaram, S. & Prakash, R. Inhibitive effect of Argemone mexicana plant extract on acid corrosion of mild Steel. *Ind. Eng. Chem. Res.* **50**, 11954–11959 (2011).
16. Soltani, N. *et al*. Silybum marianum extract as a natural source inhibitor for 304 stainless steel corrosion in 1.0 M HCl. *J. Ind. Eng. Chem.* **20**, 3217–3227 (2014).
17. Chevalier, M. *et al*. Enhanced corrosion resistance of mild steel in 1 M hydrochloric acid solution by alkaloids extract from Aniba rosaeodora plant: Electrochemical, phytochemical and XPS studies. *Electrochim. Acta* **131**, 96–105 (2014).
18. El Bribri, A., Tabyaoui, M., Tabyaoui, B., El Attari, H. & Bentiss, F. The use of Euphorbia falcata extract as eco-friendly corrosion inhibitor of carbon steel in hydrochloric acid solution. *Mater. Chem. Phys.* **141**, 240–247 (2013).
19. Garai, S., Garai, S., Jaisankar, P., Singh, J. K. & Elango, A. A comprehensive study on crude methanolic extract of Artemisia pallens (Asteraceae) and its active component as effective corrosion inhibitors of mild steel in acid solution. *Corros. Sci.* **60**, 193–204 (2012).
20. Loganayagi, C., Kamal, C. & Sethuraman, M. G. Opuntiol: an active principle of Opuntia elatior as an eco-friendly inhibitor of corrosion of mild steel in acid medium. *ACS Sustain. Chem. Eng.* **2**, 606–613 (2014).
21. Uwah, I. E., Okafor, P. C. & Ebiekpe, V. E. Inhibitive action of ethanol extracts from Nauclea latifolia on the corrosion of mild steel in H_2SO_4 solutions and their adsorption characteristics. *Arab. J. Chem.* **6**, 285–293 (2013).
22. Soltani, N., Tavakkoli, N., Khayatkashani, M., Jalali, M. R. & Mosavizade, A. Green approach to corrosion inhibition of 304 stainless steel in hydrochloric acid solution by the extract of Salvia officinalis leaves. *Corros. Sci.* **62**, 122–135 (2012).
23. Pereira, S. S. A. A. *et al*. Inhibitory action of aqueous garlic peel extract on the corrosion of carbon steel in HCl solution. *Corros. Sci.* **65**, 360–366 (2012).
24. Ji, G., Dwivedi, P., Sundaram, S. & Prakash, R. Inhibitive effect of Chlorophytum borivilianum root extract on mild steel corrosion in HCl and H_2SO_4 solutions. *Ind. Eng. Chem. Res.* **52**, 10673–10681 (2013).
25. Raja, P. B. *et al*. Evaluation of green corrosion inhibition by alkaloid extracts of Ochrosia oppositifolia and Isoreserpiline against mild steel in 1 M HCl medium. *Ind. Eng. Chem. Res.* **52**, 10582–10593 (2013).
26. Lebrini, M., Robert, F., Lecante, A. & Roos, C. Corrosion inhibition of C38 steel in 1 M hydrochloric acid medium by alkaloids extract from Oxandra asbeckii plant. *Corros. Sci.* **53**, 687–695 (2011).
27. Behpour, M., Ghoreishi, S. M., Khayatkashani, M. & Soltani, N. Green approach to corrosion inhibition of mild steel in two acidic solutions by the extract of Punica granatum peel and main constituents. *Mater. Chem. Phys.* **131**, 621–633 (2012).
28. Noor, E. A. The impact of some factors on the inhibitory action of Radish seeds aqueous extract for mild steel corrosion in 1M H_2SO_4 solution. *Mater. Chem. Phys.* **131**, 160–169 (2011).
29. Lecante, A., Robert, F., Blandinières, P. A. & Roos, C. Anti-corrosive properties of S. tinctoria and G. ouregou alkaloid extracts on low carbon steel. *Curr. Appl. Phys.* **11**, 714–724 (2011).
30. Odewunmi, N. A., Umoren, S. A. & Gasem, Z. M. Utilization of watermelon rind extract as a green corrosion inhibitor for mild steel in acidic media. *J. Ind. Eng. Chem.* **21**, 239–247 (2015).
31. Ji, G., Anjum, S., Sundaram, S. & Prakash, R. Musa paradisica peel extract as green corrosion inhibitor for mild steel in HCl solution. *Corros. Sci.* **90**, 107–117 (2015).
32. Umoren, S. A., Gasem, Z. M. & Obot, I. B. Natural products for material protection: Inhibition of mild steel corrosion by Date palm seed extracts in acidic media. *Ind. Eng. Chem. Res.* **52**, 14855–14865 (2013).
33. Abiola, O. K. & James, A. O. The effects of Aloe vera extract on corrosion and kinetics of corrosion process of zinc in HCl solution. *Corros. Sci.* **52**, 661–664 (2010).
34. Suedile, F., Robert, F., Roos, C. & Lebrini, M. Corrosion inhibition of zinc by Mansoa alliacea plant extract in sodium chloride media: extraction, characterization and electrochemical studies. *Electrochim. Acta* **133**, 631–638 (2014).
35. Gerengi, H., Schaefer, K. & Sahin, H. I. Corrosion-inhibiting effect of Mimosa extract on brass-MM55 corrosion in 0.5 M H_2SO_4 acidic media. *J. Ind. Eng. Chem.* **18**, 2204–2210 (2012).
36. Ramde, T., Rossi, S. & Zanella, C. Inhibition of the Cu65/Zn35 brass corrosion by natural extract of Camellia sinensis. *Appl. Surf. Sci.* **307**, 209–216 (2014).
37. Krishnaveni, K. & Ravichandran, J. Influence of aqueous extract of leaves of Morinda tinctoria on copper corrosion in HCl medium. *J. Electroanal. Chem.* **735**, 24–31 (2014).
38. Bozorg, M., Farahani, T. S., Neshati, J., Chaghazardi, Z. & Ziarani, G. M. Myrtus communis as green inhibitor of copper corrosion in sulfuric acid. *Ind. Eng. Chem. Res.* **53**, 4295–4303 (2014).
39. Obi-Egbedi, N. O., Obot, I. B. & Umoren, S. A. Spondias mombin L. as a green corrosion inhibitor for aluminium in sulphuric acid: Correlation between inhibitive effect and electronic properties of extracts major constituents using density functional theory. *Arab. J. Chem.* **5**, 361–373 (2012).
40. Deng, S. & Li, X. Inhibition by Jasminum nudiflorum Lindl. leaves extract of the corrosion of aluminium in HCl solution. *Corros. Sci.* **64**, 253–262 (2012).
41. Abiola, O. K., Otaigbe, J. O. E. & Kio, O. J. Gossipium hirsutum L. extracts as green corrosion inhibitor for aluminum in NaOH solution. *Corros. Sci.* **51**, 1879–1881 (2009).
42. Gerengi, H. Anticorrosive properties of Date palm (Phoenix dactylifera L.) fruit juice on 7075 type aluminum alloy in 3.5% NaCl solution. *Ind. Eng. Chem. Res.* **51**, 12835–12843 (2012).
43. Louati, S., Simmonds, M. S. J., Grayer, R. J., Kite, G. C. & Damak, M. Flavonoids from Eriobotrya japonica (Rosaceae) growing in Tunisia. *Biochem. Syst. Ecol.* **31**, 99–101 (2003).
44. Kim, J. S. *et al*. Enhancement of Eriobotrya japonica extracts on non-specific immune respons and disease resistance in kelp grouper Epinephelus bruneus against Vibrio carchariae. *Fish Shellfish Immun.* **31**, 1193–1200 (2011).
45. Cha, D. S., Eun, J. S. & Jeon, H. Anti-inflammatory and antinociceptive properties of the leaves of Eriobotrya japonica. *J. Ethnopharmacol.* **134**, 305–312 (2011).

46. Jafari, H., Danaee, I., Eskandari, H. & Rashvandavei, M. Electrochemical and theoretical studies of adsorption and corrosion inhibition of N,N′-bis(2-hydroxyethoxyacetophenone)- 2,2-dimethyl-1,2-propanediimine on low carbon steel (API 5L Grade B) in acidic solution. *Ind. Eng. Chem. Res.* **52**, 6617–6632 (2013).
47. Umoren, S. A., Li, Y. & Wang, F. H. Synergistic effect of iodide ion and polyacrylic acid on corrosion inhibition of iron in H_2SO_4 investigated by electrochemical techniques. *Corros. Sci.* **52**, 2422–2429 (2010).
48. Zheng, X., Zhang, S., Li, W., Gong, M. & Yin, L. Experimental and theoretical studies of two imidazolium-based ionic liquids as inhibitors for mild steel in sulfuric acid solution. *Corros. Sci.* **95**, 168–179 (2015).
49. Zheng, X. *et al*. Investigation of 1-butyl-3-methyl-1H- benzimidazolium iodide as inhibitor for mild steel in sulfuric acid solution. *Corros. Sci.* **80**, 383–392 (2014).
50. Zheng, X., Zhang, S., Gong, M. & Li, W. Experimental and theoretical study on the corrosion inhibition of mild steel by 1-octyl-3-methylimidazolium L-prolinate in sulfuric acid solution. *Ind. Eng. Chem. Res.* **53**, 16349–16358 (2014).
51. Al-Amiery, A. A. *et al*. Synthesis and characterization of a novel eco-friendly corrosion inhibition for mild steel in 1 M hydrochloric acid. *Sci. Rep.* **6**, 19890, https://doi.org/10.1038/srep19890 (2016).
52. Daoud, D., Douadi, T., Hamani, H., Chafaa, S. & Al-Noaimi, M. Corrosion inhibition of mild steel by two new S-heterocyclic compounds in 1 M HCl: Experimental and computational study. *Corros. Sci.* **94**, 21–37 (2015).
53. Qiang, Y. *et al*. Synergistic effect of tartaric acid with 2,6-diaminopyridine on the corrosion inhibition of mild steel in 0.5 M HCl. *Sci. Rep.* **6**, 33305, https://doi.org/10.1038/srep33305 (2016).
54. Torres, A. R., Cisneros, M. G. V. & Rodríguez, J. G. G. Medicago sativa as a green corrosion inhibitor for 1018 carbon steel in 0.5 M H_2SO_4 solution. *Green Chem. Lett. Rev.* **9**, 143–155 (2016).
55. Zheng, X., Gong, M. & Li, Q. Corrosion inhibition of mild steel in sulfuric acid solution by Houttuynia cordata extract. *Int. J. Electrochem. Sci.* **12**, 6232–6244 (2017).
56. Benali, O., Selles, C. & Salghi, R. Inhibition of acid corrosion of mild steel by Anacyclus pyrethrum L. extracts. *Res. Chem. Intermediat.* **40**, 259–268 (2012).
57. Saadawy, M. An important world crop - barley - as a new green inhibitor for acid corrosion of steel. *Anti-Corros. Method. M.* **62**, 220–228 (2015).
58. Singh, M. R., Gupta, P. & Gupta, K. The litchi (Litchi Chinensis) peels extract as a potential green inhibitor in prevention of corrosion of mild steel in 0.5 M H_2SO_4 solution. https://doi.org/10.1016/j.arabjc.2015.01.002 (2015).
59. Znini, M. *et al*. Essential oil of Salvia aucheri mesatlantica, as a green inhibitor for the corrosion of steel in 0.5M H_2SO_4. *Arab. J. Chem.* **5**, 467–474 (2012).
60. Umoren, S. A. *et al*. Inhibition of mild steel corrosion in acidic medium using coconut coir dust extracted from water and methanol as solvents. *J. Ind. Eng. Chem.* **20**, 3612–3622 (2014).
61. Sudheer, M. & Quraishi, M. A. 2-amino-3,5-dicarbonitrile-6-thio-pyridines: new and effective corrosion inhibitors for mild steel in 1 M HCl. *Ind. Eng. Chem. Res.* **53**, 2851–2859 (2014).
62. Sappani, H. K. & Karthikeyan, S. 4-chloro-2-((furan-2-ylmethyl) amino)-5-sulfamoylbenzoic acid (FSM) and n-(isopropylcarbamoyl)-4-(m-tolylamino) pyridine-3-sulfonamide (TSM) as potential inhibitors for mild steel corrosion in 1 N H_2SO_4 medium. Part I. *Ind. Eng. Chem. Res.* **53**, 3415–3425 (2014).
63. Kumar, S. H. & Karthikeyan, S. Torsemide and furosemide as green inhibitors for the corrosion of mild steel in hydrochloric acid medium. *Ind. Eng. Chem. Res.* **52**, 7457–7469 (2013).
64. Yadav, D. K., Quraishi, M. A. & Maiti, B. Inhibition effect of some benzylidenes on mild steel in 1 M HCl: An experimental and theoretical correlation. *Corros. Sci.* **55**, 254–266 (2012).
65. Kumar, S., Sharma, D., Yadav, P. & Yadav, M. Experimental and quantum chemical studies on corrosion inhibition effect of synthesized organic compounds on N80 steel in hydrochloric acid. *Ind. Eng. Chem. Res.* **52**, 14019–14029 (2013).
66. Chen, F. X., Liu, X. H. & Chen, L. S. Developmental changes in pulp organic acid concentration and activities of acid-metabolising enzymes during the fruit development of two loquat (Eriobotrya japonica Lindl.) cultivars differing in fruit acidity. *Food Chem.* **114**, 657–664 (2009).
67. Cao, J., Peng, L. Q. & Xu, J. J. Microcrystalline cellulose based matrix solid phase dispersion microextration for isomeric triterpenoid acids in loquat leaves by ultrahigh-performance liquid chromatography and quadrupole time-of-flight mass spectrometry. *J. Chromatogr. A* **1472**, 16–26 (2016).
68. Li, E. N., Luo, J. G. & Kong, L. Y. Qualitative and quantitative determination of seven triterpene acids in Eriobotrya japonica Lindl. by high-performance liquid chromatography with photodiode array detection and mass spectrometry. *Phytochem. Analysis* **20**, 338–343 (2009).
69. Aziz, A., Khan, I., Azam, S., Mehnaz, S. & Ahmad, B. Comparative antimicrobial, phytotoxic and heamaglutination potential of Eriobotrya japonica leaf extract and its zinc nano-particles[J]. *Pak. J. Bot.* **49**, 1917–1924 (2017).
70. Chauhan, L. R. & Gunasekaran, G. Corrosion inhibition of mild steel by plant extract in dilute HCl medium. *Corros. Sci.* **49**, 1143–1161 (2007).
71. Liu, Y., Zhang, W., Xu, C. & Li, X. Biological Activities of Extracts from Loquat (Eriobotrya japonica Lindl.): A Review. *Int. J. Mol. Sci*. **17**, https://doi.org/10.3390/ijms17121983 (2016).
72. Qa'Dan, F., Verspohl, E. J., Nahrstedt, A., Petereit, F. & Matalka, K. Z. Cinchonain Ib isolated from Eriobotrya japonica induces insulin secretion *in vitro* and *in vivo*. *J. Ethnopharmacol.* **124**, 224–227 (2009).
73. Yang, B. Y., Xia, Y. G., Dong, C. & Kuang, H. X. Chemical constituents from the flower of Datura metel. *Chin. J. Nat. Medicines* **31**, 429–432 (2008).
74. Park, J. H. *et al*. Lignans from silkworm droppings and their promotional activities on heme oxygenase-1 (HO-1). *J. Korean Soc. Appl. Bi.* **53**, 734–739 (2010).
75. Yokota, J. *et al*. Scavenging of reactive oxygen species by Eriobotrya japonica seed extract. *Biol. Pharm. Bull.* **29**, 467–471 (2006).
76. Banerjee, G. & Malhotra, S. N. Contribution to adsorption of aromatic amines on mild steel surface from HCl solutions by impedance, UV, and Raman spectroscopy. *Corrosion* **48**, 10–15 (1992).
77. Li, X., Xie, X., Deng, S. & Du, G. Two phenylpyrimidine derivatives as new corrosion inhibitors for cold rolled steel in hydrochloric acid solution. *Corros. Sci.* **87**, 27–39 (2014).
78. Solmaz, R. Investigation of corrosion inhibition mechanism and stability of Vitamin B1 on mild steel in 0.5 M HCl solution. *Corros. Sci.* **81**, 75–84 (2014).
79. Solmaz, R. Investigation of adsorption and corrosion inhibition of mild steel in hydrochloric acid solution by 5-(4-Dimethylaminobenzylidene)rhodanine. *Corros. Sci.* **79**, 169–176 (2014).

Acknowledgements

This project is supported financially by Talent Project of Sichuan University of Science & Engineering (No. 2016RCL11), National Natural Science Foundation of China (No. 21706195) and Sichuan Province Youth Science and Technology Fund (No. 2014JQ0036).

Author Contributions

X.Z. and M.G. designed the research and wrote the main manuscript text. Q.L. evaluated the inhibition performance using the electrochemical and weight loss measurements. L.G. evaluated the surface characterization and prepared Figures. All authors reviewed the manuscript and have agreed to its publication.

Additional Information

Competing Interests: The authors declare no competing interests.

Publisher's note: Springer Nature remains neutral with regard to jurisdictional claims in published maps and institutional affiliations.